

A Nernst heat theorem for nonequilibrium jump processes

Faezeh Khodabandehlou,^{1,*} Christian Maes,¹ and Karel Netočný²

¹*Instituut voor Theoretische Fysica, KU Leuven, Belgium*

²*Institute of Physics of the Czech Academy of Sciences, Prague, Czech Republic*

We generalize a version of the Third Law of Thermodynamics to nonequilibrium processes described as Markov jump dynamics on a finite connected graph. In addition to the stationary heat flux, after a small change in an external parameter, an excess heat flows into the thermal bath at temperature T during relaxation. We state conditions under which that excess heat and the nonequilibrium heat capacity vanish as $T \downarrow 0$. The interpretation is that typical relaxation paths towards dominant states do not dramatically differ from each other in their dissipated heat.

Keywords: nonequilibrium jump process, excess heat, Nernst heat theorem

I. INTRODUCTION

A standard topic of thermal physics concerns energy exchanges between a system and a heat bath as the result of changes in external parameters such as volume or temperature. Regularities emerge when these changes are quasistatic and along equilibria, and then get described by the thermodynamic laws for reversible processes. For example, the Clausius heat theorem identifies a state function, the entropy being the reversible heat by temperature, not ever decreasing for spontaneous processes in a closed and isolated system [1, 2]. That entropy for systems in thermodynamic equilibrium can be measured in terms of heat capacity or from latent heat (when temperature is unchanged), expressing the susceptibility of a system to exchange heat and store energy. As follows from Boltzmann's statistical interpretation of entropy, heat capacities thus yield crucial information about the internal degrees of freedom of an equilibrium system. To witness, the quantum revolution was much inspired by the difficulty to account in classical physics for the low-temperature behavior of specific heats [3]. The Third Law of Thermodynamics, as pioneered by Nernst

*Electronic address: faezeh.khodabandehlou@kuleuven.be

and Planck, deals explicitly with these questions, [4, 5] where Nernst's version considered the entropy to argue that at zero temperature it becomes a constant independent of any external parameter. Further conditions imply that the heat capacity must vanish with temperature [1, 6]. To make sure and in contrast with the First and Second Law, the Third Law is not always obeyed by substances and corresponding Nernst theorems therefore require nontrivial conditions, [7, 8].

Since longer it has been considered important to develop calorimetry and to find a similar general structure in the study of thermodynamic processes connecting steady states of nonequilibrium systems [9–11]. The point is not at all to formally extend the definition of entropy [12] and there is in fact no pressing need to take thermodynamic limits; rather we wish to obtain quantitative measures of the heat released or absorbed during a quasistatic relaxation to a (new) nonequilibrium condition *because of* (small) changes in control parameters even in small open systems. That need not be restricted to the context of linear irreversible thermodynamics or to close-to-equilibrium processes. Far-from-equilibrium examples within electronics are micro- or nano-scale devices like digital logic circuits with a rich collection of nonlinear dissipative effects due to quantum tunneling, current leakage, etc. [13]. Other examples include driven hopping dynamics on a lattice in contact with a phonon- or photon-bath, where the driving can be electromagnetic or optical. While the driving there can be time-dependent (like when applying an AC-field), here we imagine time-scales where the external field can be taken almost constant. The extension to truly time-dependent external driving is conceptually not different though. Finally, examples of increasing importance arise in life processes [14, 15], where the body or the cell act as thermal reservoir (albeit it not at low temperature) and the driving is mostly chemical. There in particular, reactions occur far from equilibrium and modeling with Markov jump processes becomes very relevant to understand the calorimetry of active systems [16, 17].

In driven systems the heat exchange runs against a dissipation background. In the stationary situation, work done by nonconservative forces are constantly dissipated as (Joule) heat. Changing an external parameter creates an *excess* heat in the relaxation to the new steady condition. Then, our interest should go to that excess part coming from changes in the temperature and/or other parameters defining the system dynamics [9–11].

Such an excess heat is well defined in the quasistatic regime, being essentially insensitive to the actual speed if the change is slow enough; see [11, 18–20]. The present paper is about the low-temperature behavior of that excess heat. As prime example, if the change is provoked by modifying the temperature of the environment, the excess heat (per change in temperature) is rightly called a nonequilibrium heat capacity [21–23].

Our main result of the present paper is that for a large and physically motivated class of nonequilibrium systems modeled as Markov jump processes the excess heat and the heat capacity vanish at absolute zero. We start with an illustration of the type of models and how nonequilibrium heat capacities may look like. It is continued in Appendix B. Next, we give the setup where the condition of local detailed balance is crucial. In Section IV we introduce the main player, which is the excess heat. That it vanishes at zero temperature is the subject of Section V, dealing with the extended Third Law. An example is presented in Section VI for illustrating the conditions. In Section VII, the heat capacity is taken as prime example; it vanishes at absolute zero under the conditions of our extended Nernst heat theorem. The Appendix adds more mathematical ingredients.

II. ILLUSTRATION

As possibly the simplest active system with nontrivial heat properties, Figs. 1 show the heat capacity for a two-level system with a switch. The levels are split by an amount $\varepsilon > 0$ and the transitions between them are assisted by an active force which randomly switches direction. The latter is modeled by the dichotomous noise σ_t with two values $\sigma = \pm$ and tumbling rates $k^{+-} = k^{-+} = \alpha$. The other four transitions are thermal at inverse temperature β with rates

$$\begin{aligned} k_{01}^+ &= k_{10}^- = \tau^{-1} e^{\beta\varepsilon/2} \\ k_{01}^- &= k_{10}^+ = \tau^{-1} e^{-\beta\varepsilon/2} \end{aligned} \tag{II.1}$$

where k_{01}^+ is the rate for the transition $(0+) \rightarrow (1+)$, etc. The kinetic factor $\tau = \tau(\beta)$ is a characteristic time for transitions between both levels. Detailed balance is broken as manifestly seen from the difference between the product of rates along the two opposite orientations of the (single) transition loop: $k_{01}^+ k^{+-} k_{10}^- k^{-+} = \alpha^2 \tau^{-2} e^{\beta\varepsilon}$, whereas

$$k_{10}^+ k^{+-} k_{01}^- k^{-+} = \alpha^2 \tau^{-2} e^{-\beta \varepsilon}.$$

Fig. 1(a) gives the heat capacity when τ is independent of β for $\varepsilon = \tau = 1$. Observe that whenever $\alpha \neq 0$ the heat capacity becomes massively enhanced at (very) low temperatures. When $\tau = e^{\beta \Delta}$, $\Delta > 0$, strongly depends on temperature, the heat capacity takes both positive and negative values. See Fig. 1 (right) for that case with $\Delta = 2$, and how the low-temperature behavior is very different both from the (nonequilibrium) heat-bath dynamics and from the equilibrium case, while still $C(T) \rightarrow 0$ as the temperature reaches absolute zero.

The heat capacity is calculated exactly in Appendix D, with some additional discussion.

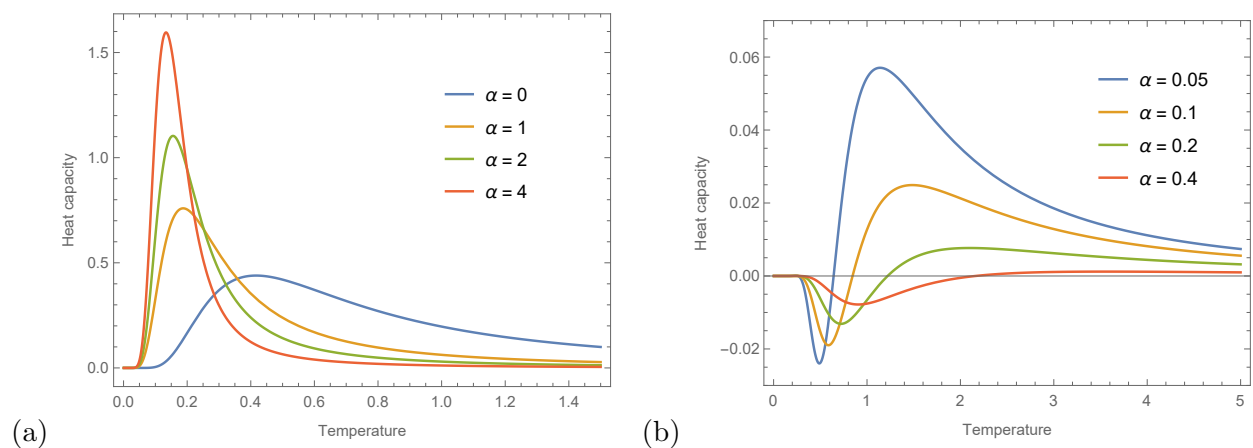


FIG. 1: Heat capacity for two-level switch, (a) without the barrier, (b) with the barrier ($\Delta = 2$).

III. SETUP

As in equilibrium, nonequilibrium extensions of Nernst heat theorem require conditions. E.g., standard driven diffusion processes are *too* classical and do not in general satisfy an extended Nernst theorem. We restrict ourselves to Markov jump processes on an (arbitrary) finite, simple and connected graph G . Vertices x, y, z, \dots denote the physical states or conditions on a mesoscopic scale of description, with energy levels $E(x)$ as for instance associated to molecules or lattice gases. The presence of an edge between vertices x, y in the graph signifies the possibility of a transition. The transition rate $k(x, y)$ for a jump

$x \rightarrow y$ contains kinetic and thermodynamic information summarizing the weak coupling of the system to a low-temperature bath. The rates are taken to satisfy local detailed balance [24],

$$\log \frac{k(x, y)}{k(y, x)} = \beta q(x, y) \quad (\text{III.1})$$

where the antisymmetric $q(x, y) = -q(y, x)$ is the heat dissipated in the thermal bath at inverse temperature β .

We imagine that the transition rates depend on a (multi-dimensional) parameter λ which physically represents the dependence of the rates on temperature T and other controls such as volume or work-functions. Every function of the transition rates thus depends on that λ , and take a subscript to specify that control. For example, the dissipated power or heat flux into the thermal bath is expected to be

$$\mathcal{P}_\lambda(x) = \sum_y k_\lambda(x, y) q_\lambda(x, y) \quad (\text{III.2})$$

when in state x . By convexity from (III.1), it has strictly positive expectation for a driven system, corresponding to Joule heating and thus mimicking the Second Law.

IV. EXCESS HEAT

The notion of excess heat has evolved from studies including [9–11] about processes connecting different nonequilibrium situations. Small changes $\lambda \rightarrow \lambda'$ change the nonequilibrium condition.

Suppose now that at an initial time $t = 0$, λ (e.g. the temperature of the thermal bath or the energy gaps in the system) slightly changes. If the change is at time zero, we get an excess heat, called quasipotential

$$V_{\lambda'}(x) = \int_0^\infty dt [\langle \mathcal{P}_{\lambda'}(X_t | X_0 = x) \rangle_{\lambda'} - \langle \mathcal{P}_{\lambda'} \rangle_{\lambda'}] \quad (\text{IV.1})$$

where expectations refer to relaxation, resp. stationarity under the nonequilibrium process for control λ' in (III.2). The time-integral converges by well-known results on finite-state Markov processes. The excess heat towards the system is then $Q_{\lambda'}^{\text{exc}}(x) = -V_{\lambda'}(x)$ when starting in state x .

We draw x from the initial stationary distribution (at time zero) at the original $\lambda = \lambda' - d\lambda$.

Taking that zero-time expectation over x we find

$$\langle Q_{\lambda'}^{\text{exc}} \rangle_{\lambda} = \langle V_{\lambda} \rangle_{\lambda} - \langle V_{\lambda'} \rangle_{\lambda}$$

where $\langle V_{\lambda} \rangle_{\lambda} = 0$. In other words, the excess heat δQ^{exc} , after a small change in an external parameter $\lambda \rightarrow \lambda' = \lambda + d\lambda$, is encoded in the (change of) V as

$$\delta Q^{\text{exc}} = -\langle dV \rangle \quad (\text{IV.2})$$

where we left out the subscripts again. Under detailed balance, $q_{\lambda}(x, y) = E_{\lambda}(x) - E_{\lambda}(y)$ and $\delta Q^{\text{eq}} = d\langle E \rangle^{\text{eq}} - \langle dE \rangle^{\text{eq}}$ as in the First Law.

Since $\langle V \rangle = 0$, we have $-\langle dV \rangle = \sum_y d\rho(y) V(y)$ where $d\rho(y)$ is the change of the (unique) stationary distribution ρ under $\lambda \rightarrow \lambda + d\lambda$. In other words,

$$\delta Q^{\text{exc}} = \sum_y d\rho(y) V(y) = \langle V ; d \log \rho \rangle \quad (\text{IV.3})$$

where $\langle f ; g \rangle = \langle fg \rangle - \langle f \rangle \langle g \rangle$ denotes the stationary covariance, and we used that $\langle d \log \rho \rangle = 0$. Note that in equilibrium, $V = E$ and $\log \rho = -\beta E - \log Z$ for the partition function Z , and the excess heat (the total heat) gets expressed in terms of the energy-variance, which assures its positivity. In nonequilibrium regimes, we get two ‘potentials’ (formally, V and $\log \rho$) and their structure and mutual correlation shape the excess heat following the response relation (IV.3).

V. THIRD LAW FOR NONEQUILIBRIUM

We understand the extended Third Law as the statement that the excess heat (as defined above for quasistatic processes between nonequilibrium conditions) vanishes at absolute zero:

$$\delta Q^{\text{exc}} \rightarrow 0 \quad (\text{V.1})$$

The right-hand side in (IV.3) depends on the temperature T via V and via ρ . In order to show (V.1), two things suffice: bounded V and $d\rho \rightarrow 0$ for $T \downarrow 0$.

That the quasipotential V is uniformly bounded at vanishing temperature is technically most complicated and, in a general setup, conditions follow from an application of the matrix-forest theorem as highlighted in Appendix C. As is clear however from (IV.1), boundedness

of V strongly relates with relaxation properties and the accessibility of the states that come to support the zero-temperature condition. A good strategy is to estimate edge-differences $V(e) = V_{\lambda'}(x) - V_{\lambda'}(y)$ for any fixed edge $e = (x, y)$ to reconstruct the function $V_{\lambda'}$. That leads to conditions that assure there is no big difference in relaxation times for the process started from x or from y . Obviously, the type of function (III.2) matters greatly; if e.g. for all edges, $q(x, y) = E(x) - E(y)$ as under global detailed balance, then $V(x) = E(x) - \langle E \rangle$ and boundedness is immediate. On the other hand, there are examples *arbitrarily close to equilibrium* where V diverges in some states. That will already be seen in the example around Fig. 2. To arrive at a formal treatment, we need more notation.

Put $\phi(x, y) = \lim_{\beta} \frac{1}{\beta} \log k(x, y)$, and we write $\phi(A) = \sum_{(x, x') \in A} \phi(x, x')$ for any set A of oriented edges. Consider the set Y of all spanning trees \mathcal{T} on the graph to put

$$\phi^* = \max_z \phi^*(z), \quad \phi^*(z) = \max_{\mathcal{T} \in Y} \phi(\mathcal{T}_z) \quad (\text{V.2})$$

where \mathcal{T}_z is the oriented tree obtained from \mathcal{T} by directing it toward z . The maximizing z are the dominant states, as follows from the low-temperature Kirchhoff formula; see [25] and (A.1) in Appendix A. As we will see, ϕ^* plays an important role somewhat of an analogue to the ground state energy in equilibrium.

Denote by \mathcal{H}_e the set of all tree-loops that include the edge e in a tree. Let $H^{(e)}$ denote an undirected tree-loop-tree, created by removing the edge e from a tree-loop $H \in \mathcal{H}_e$. For an example, we may look at Fig. 2, but see also Appendix B. Finally, $O(H^{(e)})$ is the set of all oriented tree-loop-tree's obtained by giving all possible orientations to $H^{(e)}$ (A directed tree-loop-tree is a loop with two possible directions — clockwise and counter-clockwise — and the trees connected to the loop must be toward the loop. Any separated tree is a rooted tree and all states in this tree are allowed to be a root). On the right in Fig. 2 we see both elements of $O(H^{(e)}) = \{\bar{H}_1, \bar{H}_2\}$ for $e = \{u, w\}$.

Proposition 1: $V(e)$ is uniformly bounded in β when for all $\bar{H} \in O(H^{(e)})$,

$$\phi(\bar{H}) \leq \phi^*$$

We next give another and perhaps more physical meaning to that condition, by decomposing $\phi(\bar{H}) = \phi(L + \tau) + \phi(\bar{H} \setminus L) - \phi(\tau)$ where L is the unique loop in H so that $H \setminus L$ is a collection of trees, and τ are all the edges in the trees of H which we direct towards the

loop. We take the orientation of the loop so that the current in that loop is positive; it has the asymptotics $J(L) \propto \exp(\beta(\phi(L + \tau) - \phi^*))$; see again Appendix C.

Proposition 2: $V(e)$ is uniformly bounded when for all $\bar{H} \in O(H^{(e)})$,

$$\frac{1}{\beta} \log J(L) \leq \phi(\tau) - \phi(\bar{H} \setminus L)$$

In other words, the tree-part governed by $\phi(\tau) - \phi(\bar{H} \setminus L)$ should be sufficiently large. We illustrate that in the example below of Fig. 2. —See the Appendix C for a proof of the Propositions, starting with an expression for quasipotential V obtained from the matrix-forest theorem.

Secondly, we need that $d\rho \rightarrow 0$. The vanishing of $d\rho$ at zero temperature follows from smoothness, assuming that the derivative in λ and the limit $T \downarrow 0$ can be exchanged, together with the assumption that there is a unique state x^* on which the stationary distribution gets supported: if $\rho(x) \rightarrow \delta_{x,x^*}$ for the same x^* in a neighborhood of λ , then indeed $d\rho \rightarrow 0$. A unique zero-temperature state is however compatible with multiple dominant states; see under (V.2) and in [25]. If there is a unique dominant state (in the sense that all other states are suppressed by $O(e^{-\tilde{\varepsilon}\beta})$ for some $\tilde{\varepsilon} > 0$), then the convergence for $T \downarrow 0$ is exponentially fast. If there are multiple dominant states x_i^* , then the convergence $d\rho \rightarrow 0$ may be polynomially in temperature. The dependence of the low-temperature excess heat on the behavior of the stationary condition ρ is an important instance of how heat, also in nonequilibrium statistical mechanics, informs about low-temperature degeneracy, extending the connection between Clausius and Boltzmann approaches to entropy.

VI. EXAMPLE

The physical interpretation of both Propositions can be understood by considering a realistic low-temperature asymptotics for the transitions of the system weakly coupled to e.g. a phonon bath:

$$k(x, x') = \frac{\Gamma}{|1 - e^{-\beta q(x, x')}|}$$

for $q(x, x') = E(x) - E(x') + W(x, x')$ where $W(x, x')$ is the work done by the external driving, with asymptotics

$$\begin{aligned}\phi(x, x') &= 0 \quad \text{when} \quad q(x, x') \geq 0 \\ &= q(x, x') \quad \text{when} \quad q(x, x') < 0\end{aligned}\tag{VI.1}$$

Consider Fig. 2.

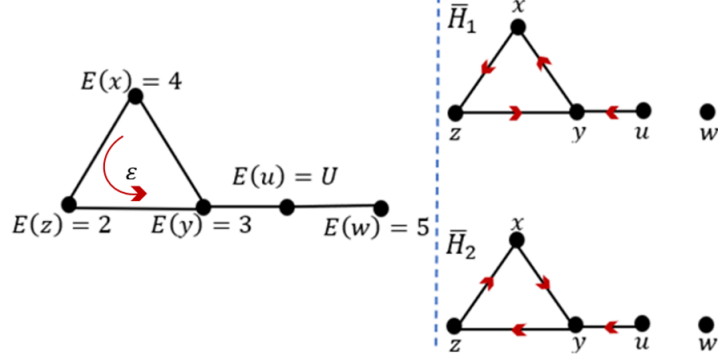


FIG. 2: Example of tree-loop; removing the edge $\{u, w\}$ gives a tree-loop-tree which can have two possible directions (notice that a vertex can be considered as a rooted tree).

We suppose frequency $\Gamma = 1$ and the specific energy landscape indicated there and, additionally, a counter-clockwise constant driving of strength $\varepsilon = 1/4$ is applied around the triangle (loop). For energy $E(u) = U \geq 5$, we find

$$\phi(x, z) = 0, \quad \phi(z, y) = -1 + \varepsilon = -3/4, \quad \phi(y, x) = -1 + \varepsilon = -3/4, \quad \phi(y, u) = 3 - U, \quad \phi(u, w) = 0,$$

$$\phi(z, x) = -2 - \varepsilon = -9/4, \quad \phi(y, z) = 0, \quad \phi(x, y) = 0, \quad \phi(u, y) = 0, \quad \phi(w, u) = 5 - U$$

to give the low-temperature asymptotics $k(e) \simeq \exp \beta \phi(e)$ for the rates over edge e . We consider two possible values $U = 10$ and $U = 5$, and we focus on the edge $e = (u, w)$ so that $O(H^{(e)}) = \{\bar{H}_1, \bar{H}_2\}$ has two elements shown in Fig. 2.

$$\phi(\bar{H}_1) = -2 + 2\varepsilon = -3/2, \quad \phi(\bar{H}_2) = -2 - \varepsilon = -9/4$$

Case $U = 10$: we find $\phi^* = -5$. In fact, in this case the quasipotential is indeed not bounded.

Case $U = 5$: we find $\phi^* = 0$ which means that $V(u) - V(w)$ remains bounded for $U = 5$ (Proposition 1).

For applying Proposition 2 with $U = 10$, we need

$$\phi(L + \tau) = -7 + 2\varepsilon, \quad \phi(\bar{H}_1 \setminus L) = \phi(\bar{H}_2 \setminus L) = 0, \quad \phi(\tau) = -5$$

and the current $J(L) \simeq e^{(-2+2\varepsilon)\beta}$ while $\phi(\tau) - \phi(\bar{H}_{1,2} \setminus L) = -5$. A physical interpretation is to say that there is a trap over the edge (w, u) when U is too large, with a delay time for relaxation which is too big for the quasipotential in $V(w)$ to be bounded.

When $U = 5$,

$$\phi(L + \tau) = -2 + 2\varepsilon, \phi(\bar{H}_1 \setminus L) = \phi(\bar{H}_2 \setminus L) = 0, \phi(\tau) = 0$$

and the current remains $J(L) \simeq e^{(-2+2\varepsilon)\beta}$ while $\phi(\tau) - \phi(\bar{H}_{1,2} \setminus L) = 0$ and the condition of Proposition 2 is satisfied.

In this example, the state z is the unique dominant state and the zero-temperature distribution gets concentrated on it.

VII. HEAT CAPACITY

Theory and basic examples of nonequilibrium heat capacities have started with [21, 22]. The heat capacity measures the excess heat *towards* the system per temperature ($= \lambda$ in that case) change. The point of departure is just (IV.2) but the change in λ is now a change in temperature $T \rightarrow T' = T + dT$, while we fix other controls such as the energy levels (as for fixed volume specific heats).

Dividing then (IV.2) by dT , we get the (constant volume) heat capacity

$$C(T) = -\left\langle \frac{d}{dT} V \right\rangle_T \quad (\text{VII.1})$$

As a consequence of the general analysis (and conditions) above, the heat capacity needs to vanish at zero temperature as well, $C(T \downarrow 0) \rightarrow 0$. The heat capacity goes to zero exponentially fast in $T \downarrow 0$ in the case of a unique dominant state and possibly much slower due to the presence of more than one dominant state. That is how the nonequilibrium heat capacity, similar to its equilibrium counterpart, reveals the support of the zero-temperature distribution.

VIII. CONCLUSIONS

For nonequilibrium systems, the excess heat measures the heat given to the system during and because of quasistatic relaxation to a nearby nonequilibrium condition. It naturally

defines a nonequilibrium heat capacity.

Considering Markov jump processes on a general finite and connected graph with rates which realistically model low-temperature transitions, we have defined the excess heat in the quasistatic relaxation to a new nonequilibrium condition. That excess heat is a product of the quasipotential V and the change $d\rho$ in stationary probabilities. An extended Nernst heat theorem starts by specifying conditions on the rates so that V is uniformly bounded as the temperature reaches absolute zero. Combined with the structure of the low-temperature asymptotics of the stationary distribution and the existence of a unique zero-temperature invariant distribution, we find that the nonequilibrium excess heat vanishes at absolute zero, exponentially or polynomially depending on having a unique or multiple dominant states. Measuring nonequilibrium heat capacities is a newer challenge, [26–31]. As explained in [17, 23], an AC-calorimetric scheme should work perfectly well and we hope the present work motivates further experimental work on low-temperature calorimetry for out-of-equilibrium systems.

Appendix A: Mathematical ingredients

We collect here mathematical ingredients, essential for the derivation of the nonequilibrium Nernst heat theorem. More details make the subject of a separate paper [32], in particular for the derivation of the graphical representations starting with the matrix-forest theorem [33–35]. For an introduction to graphical methods for nonequilibrium purposes, see [36].

We consider a simple finite and connected graph $G(\mathcal{N}, \mathcal{E})$. A random walker in continuous time has transition rates $k(x, y) > 0$ for the jumps over oriented edges $(x, y) : x \rightarrow y$ (where $x, y \in \mathcal{N}(G)$; $e : \{x, y\} \in \mathcal{E}(G)$). They satisfy local detailed balance in (III.1). They define a Markov jump process X_t having a unique (mostly unknown) stationary probability distribution ρ , with averages denoted by $\langle g \rangle = \sum_x g(x)\rho(x)$, solution of the Master equation

$$\sum_y [k(x, y)\rho(x) - k(y, x)\rho(y)] = 0, \quad \text{for all vertices } x$$

There is a Kirchhoff formula for the stationary distribution ρ , see e.g. [25, 36] for physical interpretations as well. The formula reads

$$\rho(x) = \frac{w(x)}{W}, \quad w(x) = w(\mathcal{T}_x) = \prod_{(y, y') \in \mathcal{T}_x} k(y, y') \quad (\text{A.1})$$

for normalization $W = \sum_x \sum_{\mathcal{T}_x} w(\mathcal{T}_x)$, and where \mathcal{T}_x is a spanning tree directed towards vertex x . Dominant states maximize $\Phi(x)$ in the low-temperature asymptotics $\rho(x) \simeq \exp \beta \Phi(x)$.

1. Quasipotential

In the equilibrium case, the heat $q(x, y) = q_{\text{eq}}(x, y) = E(x) - E(y)$ is entirely given in terms of the energy (potential) E , the stationary process is reversible with $\rho(x) = \rho_{\text{eq}}(x) \propto e^{-\beta E(x)}$, and satisfies (global) detailed balance with environment inverse temperature β . There is no stationary heat flux then,

$$\mathcal{P}_{\text{eq}} = \sum_x \rho_{\text{eq}}(x) \sum_y k_{\text{eq}}(x, y) [E(x) - E(y)] = 0$$

Yet, when starting in x the total heat dissipated in the thermal bath equals

$$E(x) - \langle E \rangle_{\text{eq}} = \int_0^\infty dt \sum_y \langle k_{\text{eq}}(X_t, y) [E(X_t) - E(y)] | X_0 = x \rangle_{\text{eq}}$$

That relation can be generalized to systems satisfying local detailed balance by introducing the quasipotential

$$V(x) = \int_0^\infty dt \left\{ \sum_y \langle k(X_t, y) q(X_t, y) | X_0 = x \rangle - \mathcal{P} \right\} \quad (\text{A.2})$$

where $\mathcal{P} = \sum_{x,y} \rho(x) k(x, y) q(x, y) \geq 0$ is the stationary dissipated power. That quasipotential gives the excess heat (IV.1). Note that (A.2) implies

$$\sum_y k(x, y) [V(y) - V(x) + q(x, y)] = \mathcal{P} \quad (\text{A.3})$$

while (A.3) also implies (A.2) when adding the condition that $\langle V \rangle = 0$. Obviously and in contrast with the situation for detailed balance, the quasipotential in general depends nontrivially on β . What follows next is an outline of the proof when and why V remains uniformly bounded in $\beta \uparrow \infty$.

2. Geometry and notation

We need some definitions from graph theory to present a graphical representation of the quasipotential. A *spanning subgraph* of G is a graph including all vertices of G . A *tree* is a connected subgraph without loops. A *spanning tree* is often denoted by \mathcal{T} . A *rooted tree* is an oriented tree having all its edges toward a given vertex called root; \mathcal{T}_x is a spanning tree with root x . A *tree-loop* is made by one loop L to which trees are joined ending at a vertex on the loop. A spanning tree-loop is denoted by H ; see Fig. 3.

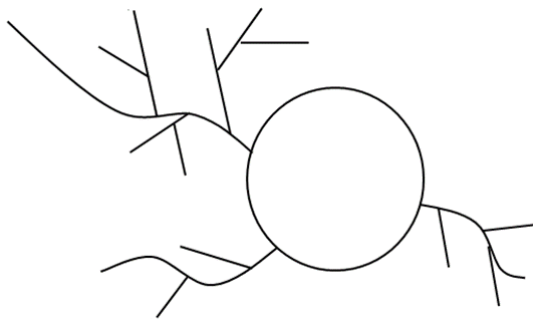


FIG. 3: A tree-loop. Any number of trees may be connected to the loop.

An *oriented tree-loop* is a tree-loop such that all edges are directed: the trees are rooted on the loop and the edges on the loop are all oriented clockwise or all counter-clockwise. See Fig.4

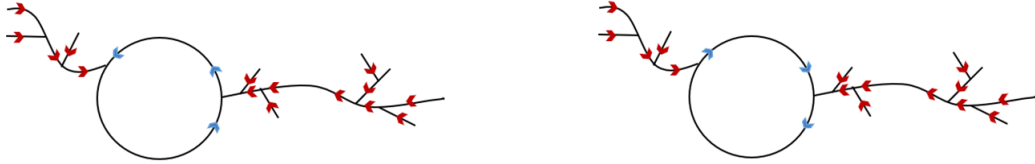


FIG. 4: Oriented tree-loop, the trees are rooted on the loop and the loop can be in two different directions.

A *tree-loop-tree* is a graph including a tree-loop and a separated tree. An oriented *tree-loop-tree* is made by an oriented tree-loop and a rooted tree. See Fig. 5.

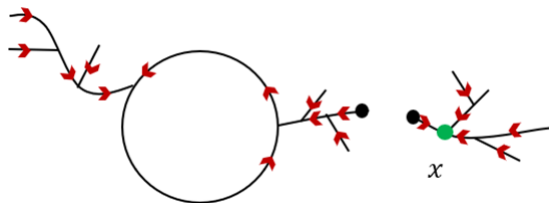


FIG. 5: An oriented tree-loop-tree when the loop is counter-clockwise.

Consider a tree-loop H_e which includes a certain edge e in the tree-part. If we remove that edge e , then a tree-loop-tree is obtained; see Fig. 6. That tree-loop-tree is denoted by $H^{(e)}$.

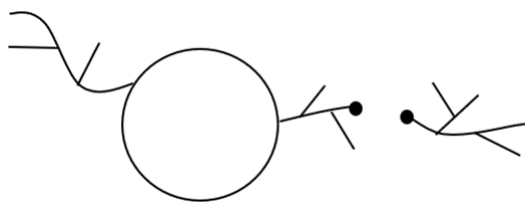


FIG. 6: A tree-loop-tree is made by removing one edge from a tree-loop.

For every $H^{(e)}$ there are different possible orientations (the tree-loop part has two possible directions of the loop and the tree-part has different possible roots). The set of all possible orientations of $H^{(e)}$ is denoted by $O(H^{(e)})$.

Oriented graphs obtain their weights as the product of transition rates along all edges. That is already manifest in the Kirchhoff formula (A.1).

3. Graphical representation

In [32] is derived a graphical representation for the quasipotential V starting from the matrix-forest theorem. We start by presenting that result.

Fix a directed edge $\bar{e} := (x, y)$ and write $V(\bar{e}) := V(x) - V(y)$. Then, we can show (basically by verifying (A.3)) that

$$V(\bar{e}) = V_{\text{tree}}(\bar{e}) + V_{\text{loop}}(\bar{e})$$

where the first term contains the weights of rooted spanning trees,

$$V_{\text{tree}}(\bar{e}) = \frac{1}{W} \sum_z \sum_{\mathcal{T}_z} w(\mathcal{T}_z) q_{\mathcal{T}}(x \rightarrow y),$$

and $q_{\mathcal{T}}(x \rightarrow y)$ sums all $q(z, z')$ with (z, z') located on the path connecting x to y on the undirected tree \mathcal{T} . The second term is

$$V_{\text{loop}}(\bar{e}) = \frac{1}{W} \sum_{H \in \mathcal{H}_e} \sum_{\bar{H} \in O(H^{(e)})} \sigma_H q(L_{\bar{H}}) w(\bar{H}) \quad (\text{A.4})$$

where \mathcal{H}_e is the set of all tree-loop's H having the edge e in a tree. $H^{(e)}$ denotes an undirected tree-loop-tree created by removing the edge e from the tree-loop H . $O(H^{(e)})$ is the set of all oriented tree-loop-tree's giving all possible directions to $H^{(e)}$ and \bar{H} denotes an element of the set $O(H^{(e)})$. (Remember that a directed tree-loop-tree is a loop with two possible directions clockwise and counter-clockwise and trees connected to the loop must be toward the loop. The separated tree is a rooted tree and all states in this tree are allowed to be a root). $L_{\bar{H}}$ is the oriented loop in \bar{H} and $q(L_{\bar{H}}) = \sum_{(z, z') \in L_{\bar{H}}} q(z, z')$. Finally, $\sigma_H = +1$ if the starting state of \bar{e} is closer to the loop and otherwise, $\sigma_H = -1$. Note that if $\mathcal{H}_e = \emptyset$ then $V(\bar{e}) = 0$. Under detailed balance, (A.4) is identically zero.

Appendix B: Example

Consider a random walker jumping on the graph G given in Fig. 7.

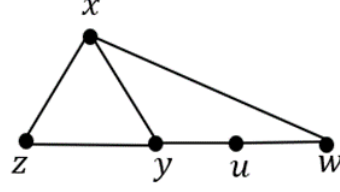


FIG. 7: Example.

We denote

$$e_1 := \{x, w\}, e_2 := \{w, u\}, e_3 := \{u, y\}, e_4 := \{y, z\}, e_5 := \{z, x\}, e_6 := \{x, y\}.$$

The graph G has six possible spanning tree-loop's, shown in Fig. 8.

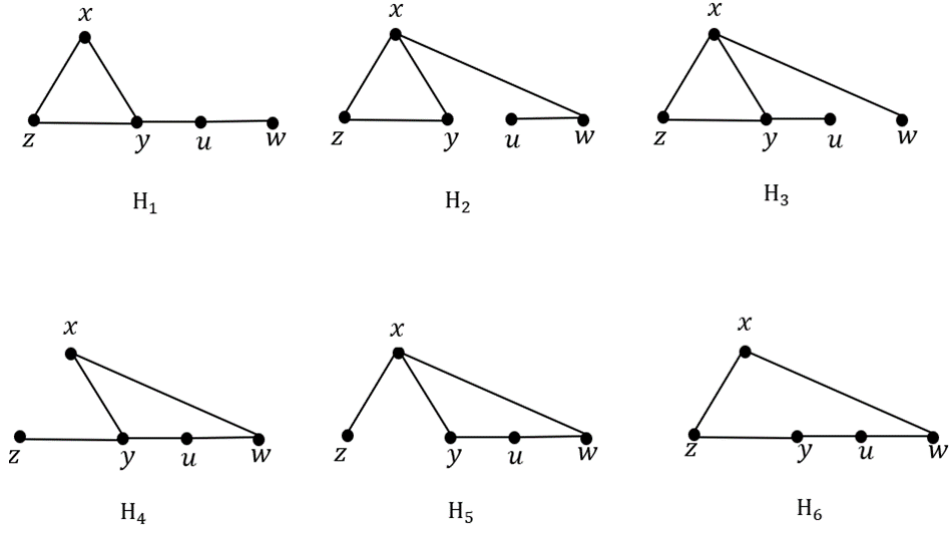
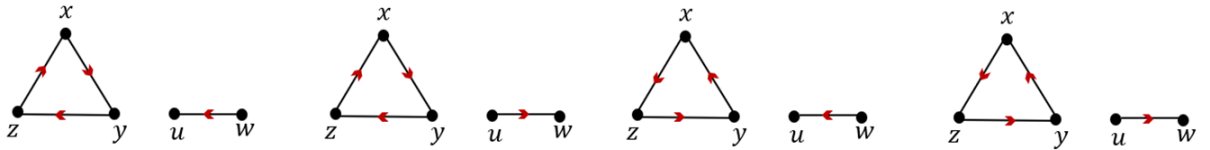


FIG. 8: All tree-loop's of the graph in Fig. 7

For every edge a set of spanning tree-loop's exists such that all components include the edge on a tree,

$$\mathcal{H}_{e_1} = \{H_2, H_3\}, \mathcal{H}_{e_2} = \{H_1, H_2\}, \mathcal{H}_{e_3} = \{H_1, H_3\}, \mathcal{H}_{e_4} = \{H_4\}, \mathcal{H}_{e_5} = \{H_5\}, \mathcal{H}_{e_6} = \emptyset.$$

In Fig. 9 we show the set $O(H_1^{(e_3)})$ created by removing the edge e_3 from the tree-loop H_1 .

FIG. 9: The components of the set $O(H_1^{(e_3)})$.

Here we can write

$$V_{\text{loop}}(\bar{e}_3) = \frac{1}{W} \left(\sum_{\bar{H} \in O(H_1^{(e_3)})} \sigma_H q(L_{\bar{H}}) w(\bar{H}) + \sum_{\bar{H} \in O(H_3^{(e_3)})} \sigma_H q(L_{\bar{H}}) w(\bar{H}) \right)$$

Appendix C: Proofs of Propositions 1 and 2

We continue by sketching the proofs of Propositions 1 and 2.

Note that $V_{\text{tree}}(\bar{e})$ is uniformly bounded in $\beta \uparrow \infty$ because all weights of spanning trees in the numerator also appear in the denominator, while the coefficient $q_{\mathcal{T}}(x \rightarrow y)$ is bounded as well.

The proof of Proposition 1 in the paper now proceeds by estimation. The factors $q(L_{\bar{H}})$ in (A.4) are bounded. To show the boundedness of $V_{\text{loop}}(\bar{e})$, it therefore suffices to show that $w(\bar{H})/W$ is bounded. Consider a directed tree-loop-tree $\bar{H} \in O(H^{(e)})$ which is created by removing the edge e from the tree-loop H and then giving direction to the edges. Then, the asymptotic weights are

$$\lim_{\beta \rightarrow \infty} \frac{1}{\beta} \log w(\bar{H}) = \phi(\bar{H})$$

Next, define $\phi^* = \max_y \phi(\mathcal{T}_y)$. Then,

$$\lim_{\beta \rightarrow \infty} \frac{1}{\beta} \log W = \lim_{\beta \rightarrow \infty} \frac{1}{\beta} \log \sum_{\mathcal{T}, y} e^{\beta \phi(\mathcal{T}_y)} = \phi^*$$

Therefore, $V(\bar{e})$ is bounded when for all $\bar{H} \in O(H^{(e)})$, $\phi(\bar{H}) \leq \phi^*$.

The proof of Proposition 2 is a physically meaningful but sufficiently simple mathematical rewriting. The main ingredient is the additivity as in the identity $\phi(\bar{H}) = \phi(L + \tau) + \phi(\bar{H} \setminus L) - \phi(\tau)$. Here, L is the unique loop in the tree-loop H and τ contains all edges in the trees of H directed towards the loop, while $\bar{H} \setminus L$ is the collection of oriented trees. The point is that (when there is external driving) we can associate a stationary current $J(L)$ to the loop L , which *a priori* is a difference $J(L) = \rho(x)k(x, y) - \rho(y)k(y, x)$ where we take the oriented edge (x, y) on the loop L and in the direction of the driving. From the Kirchhoff formula, see e.g. [36], we get its low-temperature asymptotics

$$J(L) \simeq \exp \beta(\phi(L + \tau) - \phi^*)$$

The rest of the proof follows from rewriting the condition of Proposition 1.

Appendix D: Two-level model with a switch

We give the details on the *quantum switch*–example around equation (II.1). The control parameter λ could be any of the parameters $\beta, \varepsilon, \alpha, \tau$, and everything is exactly computable. The distribution ρ gives the stationary probabilities for the four states ($i \in \{0, 1\}, \sigma = \pm 1$) of the model,

$$\rho(0, +) = \rho(1, -) = \frac{1}{Z}(\alpha\tau + e^{-\beta\varepsilon/2}) \quad \rho(0, -) = \rho(1, +) = \frac{1}{Z}(\alpha\tau + e^{\beta\varepsilon/2}) \quad (\text{D.1})$$

with normalization $Z = 4(\alpha\tau + \cosh(\beta\varepsilon/2))$. The level occupation and the switch configuration are obviously correlated.

The heat is dissipated during transitions between levels 0 and 1. The mean instantaneous power equals

$$\mathcal{P}(0, +) = \varepsilon k_{01}^+ = \tau^{-1} \varepsilon e^{\beta\varepsilon/2}, \quad \mathcal{P}(1, +) = -\varepsilon k_{10}^+ = -\tau^{-1} \varepsilon e^{-\beta\varepsilon/2} \quad (\text{D.2})$$

$$\mathcal{P}(0, -) = -\varepsilon k_{01}^- = -\tau^{-1} \varepsilon e^{-\beta\varepsilon/2}, \quad \mathcal{P}(1, -) = \varepsilon k_{10}^- = \tau^{-1} \varepsilon e^{\beta\varepsilon/2} \quad (\text{D.3})$$

from which we find the stationary heat flux, (III.2),

$$\mathcal{P} = \frac{\alpha \varepsilon \sinh(\frac{\beta\varepsilon}{2})}{\alpha\tau + \cosh(\frac{\beta\varepsilon}{2})} \quad (\text{D.4})$$

The excess heat in (IV.1) is

$$V(0, +) = V(1, -) = \frac{(1 + e^{\beta\varepsilon})e^{\beta\varepsilon}(1 + \alpha\tau e^{-\beta\varepsilon/2})}{(1 + 2\alpha\tau e^{\beta\varepsilon/2} + e^{\beta\varepsilon})^2} \varepsilon \quad (\text{D.5})$$

$$V(0, -) = V(1, +) = -\frac{(1 + e^{\beta\varepsilon})(1 + \alpha\tau e^{\beta\varepsilon/2})}{(1 + 2\alpha\tau e^{\beta\varepsilon/2} + e^{\beta\varepsilon})^2} \varepsilon \quad (\text{D.6})$$

Applying (VI.1) yields the heat capacity,

$$C(T) = \frac{(\beta\varepsilon)^2 \cosh(\frac{\beta\varepsilon}{2}) [1 + \alpha\tau \cosh(\frac{\beta\varepsilon}{2})] - \beta\alpha \sinh(\beta\varepsilon) \partial_{\beta}\tau}{4[\alpha\tau + \cosh(\frac{\beta\varepsilon}{2})]^3} \quad (\text{D.7})$$

visualized in Fig. 1, depending on the dependence or not of τ on β . The dependence on $\alpha\tau$ becomes irrelevant in the limit $\alpha \rightarrow 0$ (infinite persistence) when it boils down to the equilibrium heat capacity,

$$\lim_{\alpha \rightarrow 0} C(\alpha) = C_{\text{eq}} = \left(\frac{\beta\varepsilon}{2}\right)^2 \cosh^{-2}\left(\frac{\beta\varepsilon}{2}\right) \quad (\text{D.8})$$

In that regime the stochastic dynamics effectively splits into two almost disconnected two-level systems (+ and -), each reaching detailed balance and exhibiting equilibrium behavior (with equal heat capacities).

(I) *Heat-bath dynamics.*

If the kinetic factor τ is temperature-independent, we see the heat capacity in Fig. 1(a). Along the curves $\alpha(\beta)\tau = x e^{\beta\varepsilon/2}$ the heat capacity goes like $C = \frac{\beta\varepsilon x}{2(1+2x)^3} [1 + O(e^{-\beta\varepsilon/2})]$, which is (asymptotically) maximal for $x^* = 1/4$ to yield $C^* = C(\beta, x^*) = \beta\varepsilon [1 + O(e^{-\beta\varepsilon/2})]/27$. Informally, for $\alpha\tau \gg 1$ (the low persistence regime) the peak is located around $\beta^*\varepsilon \simeq 2 \ln(4\alpha\tau)$ and $C^* \simeq \ln(4\alpha\tau)/27$, i.e., both the inverse temperature and height of the peak grow logarithmically with the switch rate.

For fixed α , the heat capacity has the low temperature asymptotics

$$C = \frac{1}{2}(\beta\varepsilon)^2 \alpha\tau e^{-\beta\varepsilon/2} [1 + O(e^{-\beta\varepsilon/2})] \quad (\text{D.9})$$

which can be compared to the equilibrium heat capacity $C_{\text{eq}} = (\beta\varepsilon)^2 e^{-\beta\varepsilon} [1 + O(e^{-\beta\varepsilon})]$; their ratio being $C/C_{\text{eq}} \simeq \frac{1}{2}\alpha\tau e^{\beta\varepsilon/2} \gg 1$.

In contrast, at high temperatures,

$$C = \frac{(\beta\varepsilon)^2}{4(1 + \alpha\tau)^2} [1 + O(\beta\varepsilon)^2] \quad (\text{D.10})$$

so that $C/C_{\text{eq}} \simeq (1 + \alpha\tau)^{-2}$, i.e., the heat capacity increases with persistence.

It is instructive to write the heat capacity as a correlation function,

$$C = \beta^2 \langle V\Psi \rangle^{(s)}, \quad \Psi = -\frac{\partial \log \rho}{\partial \beta} \quad (\text{D.11})$$

which generalizes the equilibrium relation between the heat capacity and the variance of energy. By virtue of symmetry, we have effectively a 2-state system with the ground state 0 and the excited state 1, so that $\bar{\rho}_0 := 2\rho_0^- = 2\rho_1^+$ and $\bar{\rho}_1 := 2\rho_1^- = 2\rho_0^+$, and analogously $\bar{V}_0 := V_0^- = V_1^+$ and $\bar{V}_1 = V_1^- = V_0^+$. Since $\langle V \rangle = 0$, there is an even simpler form,

$$C = \beta^2 \bar{\rho}_1 \bar{\Psi}_1 (\bar{V}_1 - \bar{V}_0) = \beta^2 \bar{\rho}_1 (1 - \bar{\rho}_1) \Delta\Psi \Delta V \quad (\text{D.12})$$

in terms of two (temperature-dependent) ‘‘gaps’’ $\Delta\Psi = \partial_\beta \log(\bar{\rho}_0/\bar{\rho}_1)$ and $\Delta V = \bar{V}_1 - \bar{V}_0$.

Explicitly

$$\Delta V = \frac{\varepsilon \cosh\left(\frac{\beta\varepsilon}{2}\right)}{\alpha\tau + \cosh\left(\frac{\beta\varepsilon}{2}\right)}, \quad \Delta\Psi = \frac{\varepsilon}{2} \left(\frac{e^{\beta\varepsilon/2}}{\alpha\tau + e^{\beta\varepsilon/2}} + \frac{e^{-\beta\varepsilon/2}}{\alpha\tau + e^{-\beta\varepsilon/2}} \right) \quad (\text{D.13})$$

For $\alpha \rightarrow 0$ (equilibrium) we check that $\Delta V = \Delta\Psi = \varepsilon$ as expected. For $\alpha \neq 0$ they are both always positive — note that the positivity of the correlations implies positivity of the heat capacity. Yet, the gaps ΔV and $\Delta\Psi$ are different and temperature-dependent in general. For $\beta \rightarrow \infty$ we obtain $\Delta V \rightarrow \varepsilon$, whereas $\Delta\Psi \rightarrow \varepsilon/2$. Since the latter also determines the asymptotic decay of the occupation of the excited state, we understand why the heat capacity vanishes at zero temperature as $e^{-\beta\varepsilon/2}$ while the equilibrium heat capacity vanishes as $e^{-\beta\varepsilon}$. Note also that the latter is a good approximation only as long as $\Delta\Psi$ is roughly constant, i.e., for $\beta\varepsilon \gg 2 \log(\alpha\tau)$ (i.e., not including the temperature regime of the peak). In the high-temperature regime, along $\beta \rightarrow 0$, we have $\Delta V \rightarrow \varepsilon/(1 + \alpha\tau)$ and $\Delta\Psi \rightarrow \varepsilon/(1 + \alpha\tau)$, from which the decrease of the heat capacity in the high-temperature regime follows.

(II) Arrhenius model.

For the thermally-activated process with energy barrier Δ and $\tau = e^{\beta\Delta}$, we refer to Fig. 1(b). A necessary and sufficient condition for the heat capacity to obtain negative values is

$$\Delta > \frac{\beta\varepsilon^2}{2 \tanh\left(\frac{\beta\varepsilon}{2}\right)}, \quad \alpha > \frac{(\beta\varepsilon)^2 e^{-\beta\Delta}}{2\beta\Delta \sinh\left(\frac{\beta\varepsilon}{2}\right) - (\beta\varepsilon)^2 \cosh\left(\frac{\beta\varepsilon}{2}\right)} \quad (\text{D.14})$$

In terms of the previous analysis, this anomalous behavior originates from the negative values of the gap $\Delta\Psi$ while the gap ΔV is formally the same as in the previous model with α replaced by $e^{\beta\Delta}$.

We recognize two asymptotic regimes:

- (1) $\alpha \ll e^{-\beta(\Delta-\varepsilon/2)}$ (high persistence):

$$C \simeq C_{\text{eq}} + \alpha e^{-\beta\Delta} \frac{(\beta\varepsilon)^2 - 2\beta\Delta \tanh\left(\frac{\beta\varepsilon}{2}\right)}{4 \cosh\left(\frac{\beta\varepsilon}{2}\right)} \quad (\text{D.15})$$

- (2) $\alpha \gg e^{-\beta(\Delta-\varepsilon/2)}$ (low-persistence):

$$C \simeq \frac{1}{4\alpha^2} e^{-2\beta\Delta} \left[(\beta\varepsilon)^2 \cosh^2\left(\frac{\beta\varepsilon}{2}\right) - \beta\Delta \sinh\left(\frac{\beta\varepsilon}{2}\right) \right] \quad (\text{D.16})$$

It is negative under the conditions (D.14) and it vanishes in the limit $\alpha \rightarrow \infty$.

-
- [1] H. B. Callen, *Thermodynamics and an Introduction to Thermostatistics*. Wiley; 2nd edition (January 16, 1991).
- [2] E. Fermi, *Thermodynamics*. Dover Publications; New Ed edition (June 1, 1956).
- [3] M. J. Klein, Einstein, *Specific Heats and the Early Quantum Theory*. Science, New Series, American Association for the Advancement of Science, vol (**148**), No. 3667, 173-180 (April 9, 1965).
- [4] W. Nernst, *The New Heat Theorem*. Methuen and Company, Ltd., (1926).
- [5] M. Planck, *Thermodynamik*. 3rd edn (De Gruyter, 1911).
- [6] L. Masanes and J. Oppenheim, *A general derivation and quantification of the third law of thermodynamics*. Nat. Commun. **8**, 14538 (2017).
- [7] E.H. Lieb, *Residual Entropy of Square Ice*. Phys. Rev. **162**, 162 (1967).
- [8] M. Aizenman and E. Lieb, *The third law of thermodynamics and the degeneracy of the ground state for lattice systems*. J. Stat. Phys. **24**, 279–297 (1981).
- [9] P. Glansdorff, G. Nicolis and I. Prigogine, *The thermodynamic stability theory of non-equilibrium states*. Proc. Nat. Acad. Sci. USA **71**, 197–199 (1974).
- [10] Y. Oono and M. Paniconi, *Steady state thermodynamics*. Prog. Theor. Phys. Suppl. **130**, 29 (1998).
- [11] T.S. Komatsu, N. Nakagawa, S.I. Sasa and H. Tasaki, *Steady State Thermodynamics for Heat Conduction – Microscopic Derivation*. Phys. Rev. Lett. **100**, 230602 (2008).
—, J. Stat. Phys. **134**, 401 (2009).
- [12] C. Maes, *Nonequilibrium entropies*. Physica Scripta **86**, 058509 (2012).
- [13] E. Pop, *Energy Dissipation and Transport in Nanoscale Devices*. Nano Res **3**, 147 (2010).
- [14] Eds. Patrick Kent Gallagher, Michael E. Brown and Richard B. Kemp, *Handbook of Thermal Analysis and Calorimetry: From macromolecules to man*, Elsevier, **4**, (1999).
- [15] Ed. Dénes Lörczy, *The nature of biological systems as revealed by thermal methods*, Volume 5 of Hot topics in thermal analysis and calorimetry, Springer, (2004).
- [16] F. Khodabandehlou, S. Krekels and I. Maes, *Exact computation of heat capacities for active particles on a graph*. In preparation.
- [17] P. Dolai, C. Maes and K. Netočný, *Active calorimetry for active systems*. In preparation.

- [18] L. Bertini, D. Gabrielli, G. Jona-Lasinio and C. Landim, *Thermodynamic transformations of nonequilibrium states*. J. Stat. Phys. **149**, 773–802 (2012).
—, *Clausius inequality and optimality of quasistatic transformations for nonequilibrium stationary states*. Phys. Rev. Lett. **110**, 020601 (2013).
- [19] K. Saito and H. Tasaki, *Extended Clausius Relation and Entropy for Nonequilibrium Steady States in Heat Conducting Quantum Systems*. J. Stat. Phys. **145**, 1275-1290 (2011).
- [20] C. Maes and K. Netočný, *A nonequilibrium extension of the Clausius heat theorem*. J. Stat. Phys. **154**, 188–203 (2014).
- [21] E. Boksenbojm, C. Maes, K. Netočný, and J. Pešek, *Heat capacity in nonequilibrium steady states*. Europhys. Lett. **96**, 40001 (2011).
- [22] J. Pešek, E. Boksenbojm, and K. Netočný, *Model study on steady heat capacity in driven stochastic systems*. Cent. Eur. J. Phys. **10**(3), 692–701 (2012).
- [23] C. Maes and K. Netočný, *Nonequilibrium Calorimetry*. J. Stat. Mech. **114004** (2019).
- [24] C. Maes, *Local detailed balance*. SciPost Phys. Lect. Notes **32**, 17pp (2021).
- [25] C. Maes and K. Netočný, *Heat bounds and the blowtorch theorem*. Annales Henri Poincaré **14**, 1193–1202 (2013).
- [26] J. K. Nielsen and J. C. Dyre, *Fluctuation-dissipation theorem for frequency-dependent specific heat*. Phys. Rev. B **54**, 15754 (1996).
- [27] M. J. de Oliveira, *Complex heat capacity and entropy production of temperature modulated systems*. arXiv:1905.10306v1 [cond-mat.stat-mech]
- [28] J. del Cerro and S. Ramos, *Specific heat of latgs ferroelectric crystal under dissipative conditions*. Ferroelectrics Letters, **16**, 119 (1993).
- [29] H. P. Leiseifer, *Heat Production and Growth Kinetics of E. coli K12 from Flow Calorimetric Measurements on Chemostat Cultures*. Z Naturforsch C J Biosci. **4**, 1036–48 (1989).
- [30] L. Hansen, R. Criddle, E. H. Battley, *Biological calorimetry and the thermodynamics of the origination and evolution of life*. Pure Appl. Chem. **81**, 1843 (2009).
- [31] S. Krishnamurthy, S. Ghosh, D. Chatterji, R. Ganapathy and A. K. Sood, *A Micrometer-sized Heat Engine Operating Between Bacterial Reservoirs*. Nature Physics **12**, 1134–1138 (2016).
- [32] F. Khodabandehlou, I. Maes and K. Netočný, *A nonequilibrium version of the Nernst heat theorem* (in preparation).
- [33] R. Agaev and P. Chebotarev, *The matrix of maximum out forests of a digraph and its appli-*

- cations*. Autom Remote Control **61**(9), 1424–1450 (2006).
- [34] P. Chebotarev and E. Shamis, *The matrix-forest theorem and measuring relations in small social groups*, Autom. Remote Control **58**, 1505, arXiv:math/0602070, (1997).
- [35] F. Khodabandehlou and I. Maes, *Drazin–Inverse and heat capacity for driven random walks on the ring*. arXiv:2204.04974v2 [math.PR].
- [36] F. Khodabandehlou, C. Maes and K. Netočný, *Trees and forests for nonequilibrium purposes: an introduction to graphical representations*. arXiv:2207.02521v1 [cond-mat.stat-mech].